



# Design of substrate label for steady state flux measurements in plant systems using the metabolic network of *Brassica napus* embryos

Igor G.L. Libourel<sup>a,\*</sup>, Jackson P. Gehan<sup>a,b</sup>, Yair Shachar-Hill<sup>a</sup>

<sup>a</sup> Department of Plant Biology, Michigan State University, East Lansing, Michigan 48824, USA

<sup>b</sup> MSU-DOE Plant Research Laboratory, Michigan State University, East Lansing, MI 48824, USA

Received 20 February 2007; received in revised form 23 April 2007

## Abstract

Steady state metabolic flux analysis using <sup>13</sup>C labeled substrates is of growing importance in plant physiology and metabolic engineering. The quality of the flux estimates in <sup>13</sup>C metabolic flux analysis depend on the: (i) network structure; (ii) flux values; (iii) design of the labeling substrate; and (iv) label measurements performed. Whereas the first two parameters are facts of nature, the latter two are to some extent controlled by the experimenter, yet they have received little attention in most plant studies. Using the metabolic flux map of developing *Brassica napus* (Rapeseed) embryos, this study explores the value of optimal substrate label designs obtained with different statistical criteria and addresses the applicability of different optimal designs to biological questions. The results demonstrate the value of optimizing the choice of labeled substrates and show that substrate combinations commonly used in bacterial studies can be far from optimal for mapping fluxes in plant systems. The value of performing additional experiments and the inclusion of measurements is also evaluated.

© 2007 Elsevier Ltd. All rights reserved.

**Keywords:** Metabolic flux analysis; Optimal design; *Brassica napus*; <sup>13</sup>C labeling

## 1. Introduction

Steady state metabolic flux analysis based on <sup>13</sup>C-isotope measurements has emerged as a powerful tool for metabolic engineering (Sauer, 2006). The statistical analysis of parameter estimation and progress in analytical and computational methods (Fischer and Sauer, 2003; van Winden et al., 2001; Wiechert et al., 1997, 1999; Wittmann and Heinzle, 2001) have given flux measurements based on isotope labeling experiments a quantitative foundation. Much of the technology for steady state labeling experiments has

been developed in the field of microbial biology and methods are tailored to metabolic studies on microbes. Quantitative steady state flux studies are now also routinely applied to plant systems, and metabolic flux maps have been determined for various tissues and plant species (Ratcliffe and Shachar-Hill, 2006; Schwender et al., 2004b). Amongst the most popular model systems are embryo cultures due to the economical importance of seed filling.

Although experimental design studies for optimal substrate label have been performed for microbial experiments (Arauzo-Bravo and Shimizu, 2003; Mollney et al., 1999; Wittmann and Heinzle, 2001), the results of these studies cannot be assumed to be applicable to plants. The combined differences in network structure, carbon substrate and flux values suggest that a good substrate label design for a bacterial strain may be a poor one for a developing plant embryo. This has been acknowledged and *ad hoc* label designs have been used to compensate for the differences

*Abbreviations:*  $\chi^2$ , chi-squared;  $\sigma^2$ , variance;  $\sigma$ , standard deviation;  $\bar{\sigma}$ , geometric mean of  $\sigma$ ;  $\bar{\sigma}$ , arithmetic mean of  $\sigma$ ;  $\hat{\theta}$ , flux estimates at regression solution;  $\theta$ , flux parameter values;  $\Sigma$ , measurement covariance matrix.

\* Corresponding author. Tel.: +517 432 7120; fax: +517 353 1926.

E-mail address: libourel@msu.edu (I.G.L. Libourel).

(Schwender et al., 2004b). In this study a more systematic approach is taken by using established experimental optimality criteria.

An optimal design is a practical adaptation of an experiment to gain the most precise information about the question pursued. Within the limitations of feasible measurements and available substrates, the experimenter must decide how much, and which, additional information is required or even desirable. The measurements of label distribution in metabolites report on fluxes with different sensitivity depending on the labeled substrate supplied. The same metabolite measurement can therefore be used to provide information about different fluxes, but sensitivity gained for one flux often means sensitivity lost for another. In other words: each particular substrate label design provides a unique *view* of the flux values projected onto the metabolites. This perspective implies that multiple experiments, using a different substrate labeling each time, allow the experimenter to gain additional information about the flux values.

As an experimental design depends on the true flux values, an optimal experiment can only be designed when the flux values are known. However, flux values are good estimates at best, and are not obtained until after flux analysis. It follows that an iterative approach is needed (Mollney et al., 1999). A rough first experiment can be used to refine the choice of label for a next, more sensitive experiment and so on.

To compare experimental designs a numerical quality score should be generated for each one. Such a quality score is calculated based on a chosen statistical criterion and the most suitable criterion depends on the aims of the experimental design. A family of such criteria, with matching aims, is known from experimental design theory (Pázman, 1986; Pukelsheim, 1993). A-, D- and E-criteria are popular choices in design theory and are suitable criteria for the aims of this study. A- and D-criterion values are related to the arithmetic mean  $\sigma^2$  and geometric mean  $\sigma^2$  of the flux estimates respectively as explained in Section 4. The meaning of the E-criterion value itself can not be interpreted so readily because it represents the largest eigenvalue of the covariance matrix, which does not relate to flux errors directly. It follows that an A-optimal design will have the smallest mean flux  $\sigma^2$ , a desirable property if the aim is to refine the exact flux values of an already well-known flux map. A D-optimal design minimizes the total variance in the system and has the attractive property of a relative low sensitivity to change in flux values, but may lead to a design that gives several large flux  $\sigma^2$  values (see Section 4). Finally the E-criterion tends to reduce the largest flux  $\sigma^2$  values, which is an attractive asset if an even coverage of the flux map is desired, such as for a mutant screen. A partial optimal design aims at getting the best estimate of one or several selected fluxes, while disregarding others that are of less interest to the investigator. This situation can arise when a specific biological question is addressed.

This optimal design study is guided by two practical objectives of biological interest. The first objective was to

find a general labeling strategy for experiments that best describes the metabolic fluxes of *Brassica napus* embryos. The optimal labeling recipe can consequently be applied to improve the precision of the flux map and be used for general mutant screens. The second objective is to find a tailored labeling strategy to most precisely describe the carbon balance of the upper part of the flux map (above phosphoenolpyruvate). This question is of interest because it directly relates to the carbon conversion efficiency, which is a measure of the relative efficiency in which captured carbon is converted into oil or lost as CO<sub>2</sub> (Goffman et al., 2005; Schwender et al., 2004a).

Five differently labeled forms of <sup>13</sup>C-glucose, as well as two forms of each of the amino acids glutamine and alanine are considered as substrates.

The effects of additional measurements recently employed in our laboratory (Allen et al., 2007) as well as the information gained by performing multiple experiments (Schwender et al., 2006) are considered. We demonstrate that simulations which simultaneously consider the design of multiple experiments allows for better estimates of the fluxes than do single experiments or multiple experiments designed sequentially. The relative benefits of two statistical optimality criteria (A and D) are investigated in depth.

### 1.1. Model description and statistical analysis

The stoichiometry of a metabolic network is defined by mass balance equations around the internal metabolites. The number of fluxes less the number of independent relationships between the fluxes is known as the degree of underdeterminacy. To make the stoichiometric matrix determined a subset of the fluxes is estimated and substituted into the metabolite balance equations. Following the nomenclature of Wiechert and co-workers these fluxes are referred to as free or constrained. Constrained fluxes are for instance irreversible enzyme steps (reverse flux is set to zero) and for this model, so are fluxes to biomass. All other fluxes are determined through their relationships to these fluxes via the stoichiometric matrix and are referred to as dependent fluxes (Wiechert and de Graaf, 1997). Because the entire flux map is determined by just the free fluxes, they also form a complete description of the variance of the system (Mollney et al., 1999). Calculations of general optimality criteria are therefore based on the free flux covariance matrix rather than the full covariance matrix. However, the selection of free fluxes is arbitrary and variances of dependent fluxes can be inferred from the free flux variances. The parameter estimates  $\hat{\Theta}$  are obtained by minimizing the difference between measured and calculated measurements. This involves using the directly measured fluxes  $w$ , the label measurements expressed as cumomers  $y$ , the measurement errors  $\Sigma_w$  and  $\Sigma_y$  and the scaling factors  $\omega$ :

$$\min_{\Theta, \omega} \left\| F_w(\Theta) - w \right\|_{\Sigma_w}^2 + \left\| F_y(\Theta, \omega) - y \right\|_{\Sigma_y}^2$$

In the equation,  $F_w$  and  $F_y$  are the simulated flux measurements and cumomer expressions, respectively. Without the scaling parameters, which are not used in this experimental design study, the simplified flux covariance matrix is given by (Mollney et al., 1999; Wiechert et al., 1997):

$$\text{Cov}_\theta = \left[ \left( \frac{\partial F_y}{\partial \theta} \right)' \cdot \Sigma_y^{-1} \cdot \left( \frac{\partial F_y}{\partial \theta} \right) \right]^{-1}$$

Solving the Jacobian  $\left( \frac{\partial F_y}{\partial \theta} \right)$  analytically (Mollney et al., 1999) yields the flux covariance matrix directly. The quality of the statistical features of an experimental design is evaluated using properties of the covariance matrix and is expressed as a criterion value (see Section 4). The measurement sensitivity matrix expresses the changes in measurements resulting from a small change in flux weighted by the measurement  $\sigma$ 's (Wiechert et al., 1997). The parameter sensitivity matrix is defined as the (pseudo) inverse of the measurement sensitivity matrix. For reasons of simplicity,  $\sigma$  values are used directly and not converted to confidence intervals.

### 1.2. Information content and optimal designs

Scaling of criterion values makes it possible to interpret a change in criterion value as a change in mean  $\sigma$ . However, evaluating the different criteria for a particular design will not result in identical numbers, but the relative improvement from one design to another can be compared on the scale of  $\sigma$ . To do this, Mollney et al. (1999) introduced the information parameter  $I_{\text{Dcrit}}$  which compares a design to a reference experiment using the D-criterion values.

$$I_{\text{crit}} = \frac{\text{crit}}{\text{crit}_{\text{reference}}}$$

This concept is here applied for all criteria  $I_A$ ,  $I_D$  and  $I_E$  as well as for a direct comparison of the  $\bar{\sigma}$  using  $I_\sigma$ .

An optimal design is defined as the substrate combination resulting from a minimization of a criterion value. Hence an A-optimal design is obtained by minimizing the A-criterion value, but also has a D- and an E-criterion value as well as a relative change in information content according to the information parameters. An improvement of a label design compared to the reference experiment corresponds to an information value smaller than 1.

## 2. Results and discussion

### 2.1. Comparison of optimal substrate designs

Besides glucose and sucrose, *B. napus* embryos consume alanine and glutamine. This study therefore investigated optimal labeling designs that incorporate five different glucose isotopomers and uniformly labeled and unlabeled forms of the two amino acids (Table 1). The choice of glu-

cose isotopomers was based on commercial availability, price and historic usage Fig. 1.

General optimal designs for the A-, D- and E-criterion were obtained by selection of the best solution from the results of at least 50 optimization trials for an optimality simulation experiment. The optimal labeling combinations can be readily interpreted by comparing the information content  $I_{\text{crit}}$  values. Most of the substrate combinations of the different optimal designs were very similar (Fig. 2), a feature that was predicted by optimal design theory (Pázman, 1986; Pukelsheim, 1993). Convergence of different optimal design solutions is indicative for a global optimum, but it is not possible to prove that a global minimal criterion value was found (Pázman, 1986). Though all evaluated optimalities are concave, optimizations using the A-criterion were most successful in consistently reaching a similar, low criterion value (Fig. 3). D-criterion and E-criterion (data not shown) based optimizations were less often able to find good minima (Fig. 3).

No optimal designs included singly labeled glucose (Fig. 3). This may well be a consequence of the relatively large number of mass-isotope measurements (from mass spectra) compared to NMR-based positional enrichment measurements in the measurement set (Mollney et al., 1999).

### 2.2. A-optimal designs have the smallest average $\sigma$ and $\sigma^2$

A comparison of the performance of the different optimalities is shown in Table 2. Because A-optimal designs are based on minimization of the trace of the covariance matrix, A-optimal designs were expected to have – and indeed showed – the best  $\bar{\sigma}$  when derived from the  $\sigma^2$ . A-optimal designs also resulted in the smallest  $\bar{\sigma}$  when derived from the individual flux  $\sigma$ s. This need not necessarily have been so, given that D-optimal designs also aim to minimize the total  $\sigma^2$  in the system. A larger spread between the smallest and largest  $\sigma^2$  could cause a larger arithmetic mean of  $\sigma^2$ , but a smaller  $\bar{\sigma}$ . Hence it was not surprising that the difference between information content of the two optimalities was smaller according to this evaluation.

Table 1  
<sup>13</sup>C-Label of substrates considered

Substrate name	Isotopmer
Unlabeled-glucose	oooooo
U- <sup>13</sup> C-glucose	●●●●●●
1- <sup>13</sup> C-glucose	●ooooo
1,2- <sup>13</sup> C-glucose	●●oooo
2- <sup>13</sup> C-glucose	o●oooo
Unlabeled-glutamine	oooooo
U- <sup>13</sup> C-glutamine	●●●●●●
Unlabeled-alanine	ooo
U- <sup>13</sup> C alanine	●●●

Filled circles indicate <sup>13</sup>C-label, open circles indicate natural abundance. The five glucose alternatives and the two alternatives for each of the amino acids reduce to six independent variables because the fractional labeling of each substrate has to add to one.

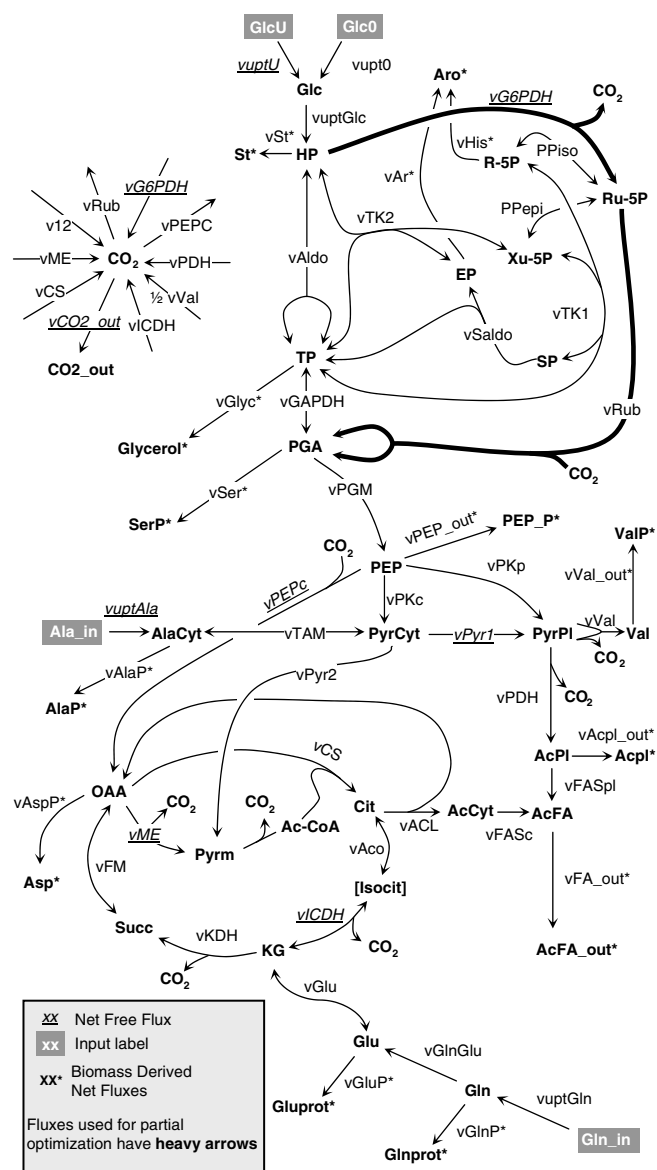


Fig. 1. Metabolic network of central metabolism in *Brassica napus* embryos during seed development showing the fluxes and metabolites used in the flux model of this study. The network consists mainly of the reactions of glycolysis, gluconeogenesis, the oxidative and reductive pentose phosphate pathways, the TCA cycle, and the syntheses of amino acids and oil. Inset is a diagram of all the fluxes producing and consuming CO<sub>2</sub>. Note how the carbon balance of the upper part of the network (above PEP) is determined by the production of CO<sub>2</sub> by the oxidative branch of the pentose phosphate pathway (vG6PDH) and the CO<sub>2</sub> consumption by rubisco. Adapted from Schwender et al. (2006).

More surprising was the observation that in some cases D-criterion based optimizations were unable to find solutions with a better D-criterion value than A-criterion based optimizations (Table 2). Rounding errors resulting from matrix manipulations used to calculate D- and E-criteria could have been responsible for premature termination of optimizations. The differences were small however, and the substrate design was very similar (Fig. 2A). E-optimal designs performed worse according to all information measures ( $I_A$ ,  $I_D$  and  $I_o$ ) and E-optimal designs were not fur-

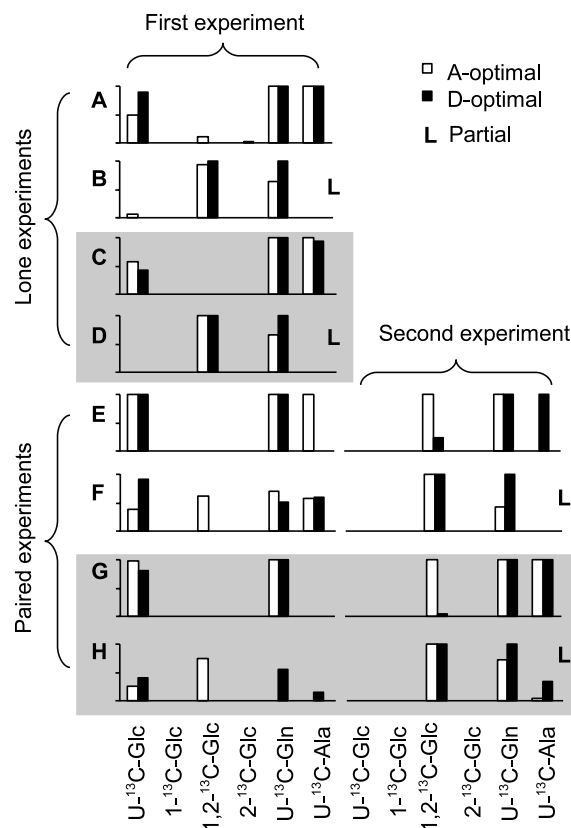


Fig. 2. Optimal mixtures of <sup>13</sup>C labeled substrates for A- and D-optimal experimental designs for the metabolic network of developing *B. napus* seeds shown in Fig. 1 using flux values through the network obtained by Schwender et al. (2006). Optimized substrate combinations were computed as described in Section 4 for either sole experiments (A–D) or paired experiments (E–H). Shaded panels describe the results of optimal designs including an extended measurement set. Experiments labeled L were partial optimal designs aimed at selectively improving the information content for two of the fluxes: vG6PDH and vRub. Only the labeled substrates are shown because the unlabeled substrates complete the substrate fractions. Scales are fractional (0–1).

ther pursued in depth. Note that the well-known AM–GM inequality between the geometric and arithmetic mean  $(a_1 + \dots + a_N)/N \geq (a_1 \cdot \dots \cdot a_N)^{1/N}$  was larger for the D-optimal design than for the A-optimal design, reflecting the needle shape of the confidence ellipsoid from D-criterion optimizations (see Section 4). Unlike in the example in Table 2, E-optimal designs often resulted in the smallest AM–GM inequality in subsequent simulation experiments (data not shown).

### 2.3. Optimal designs greatly outperform reference experiments

All three optimal label designs compared favorably to two reference experiments taken from the literature. The two examples: 90% unlabeled and 10% uniformly-labeled glucose (Szyperki, 1995) and 90% C1-labeled and 10% uniformly-labeled glucose (Schmidt et al., 1997) were outperformed by approximately 5-fold by the A- and D-optimal designs (Table 2). This large difference could be readily

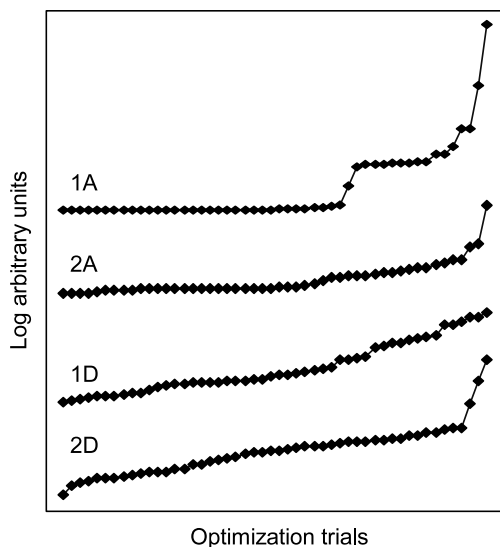


Fig. 3. Comparison of optimization performance for A- and D-criteria ranked by optimized criterion values. Each trace shows the results of 50 optimization trials starting from random initial substrate combinations. The traces of the criterion values are not shown to the same scale and no direct comparison between traces is intended. Rather the traces show whether the optimizations consistently found similar or identical criterion values, suggesting that a global optimum had been obtained. Optimizations for A-optimality (1A and 2A) more often found good global minima than did optimizations based on the D-criterion (1D and 2D). Lone experiment designs (1A and 1D) optimized more consistently than paired designs.

explained by the differences in substrate uptake, metabolic network structure and flux sizes between the biological systems considered. *B. napus* embryos take up roughly twice as much sucrose as glucose (measured in hexose units), which dilutes the label intake through glucose by threefold. In addition, the flux map of *B. napus* features photosynthesis driven re-fixation of  $\text{CO}_2$  through the rubisco bypass (Schwender et al., 2004a). This bypass provides unique labeling information about the pentose phosphate cycle through  $\text{CO}_2$  incorporation. Sensitivity to reparameterization (changes in flux values), and the inequality of the measurement sets form additional reasons why the optimal label design was so drastically different for *B. napus* compared to the reference experiments.

Table 2  
Comparison of optimal designs for sole experiments evaluated by the different optimality criteria

	Optimal design			Szyperski '95	Schmidt '98
	A	D	E		
$I_\sigma$	1.00	1.08	1.92	5.80	6.87
$I_A$	1.00	1.11	1.63	5.48	6.49
$I_D$	1.00	1.01*	1.59	5.50	3.85
$\frac{\bar{\sigma}}{\bar{\sigma}}$	5.92	6.33	7.14	6.24	10.56

The three optimal designs are shown in the first three columns and two experiments taken from the literature are shown for comparison (right-most two columns). All Information values are relative to the A-optimal design, which performed best on all information criteria including  $I_D$  (marked with \*). Note that the confidence ellipsoid of the D-optimal design is more needle-shaped than the A-optimal design ( $\bar{\sigma}/\bar{\sigma}$ ).

#### 2.4. Additional measurements and additional experiments improve information content

The effect of additional measurements that were recently implemented (Allen et al., 2007) on the determinacy of the fluxes was simulated. Only those measurements that could be added without altering the network definition were used (Table 3). The simulation results showed that the inclusion of additional measurements had little effect on substrate design (Compare Fig. 2A–C) but did increase the information content (both  $I_D$  and  $I_A$ ) by a factor of 1.5 (data not shown).

The information content was further enhanced by performing a second (paired) experiment. Because multiple experiments allowed for multiple labeling strategies, the size of the measurement set was effectively multiplied by the number of experiments. Note that if no valuable alternate labeling options exist, experiments become redundant and no additional information is gained. A second labeling experiment however, increased the information by a factor of 1.7 and the use of two experiments combined with the extended measurement dataset lead to an overall gain of 2.4 (data not shown). The relative improvement for the different experimental scenarios is illustrated for the two fluxes vG6PDH and vRub in Fig. 4.

#### 2.5. Optimal designs of paired experiments

Simultaneous optimizations of substrates for paired experiments lead to higher amounts of  $\text{U-}^{13}\text{C}$ -glucose in one of the experiments and a high contribution of  $1,2\text{-}^{13}\text{C}$ -glucose in the other (compare Fig. 2A–E and B–F). The use of label in alanine was reduced, especially in combination with uniformly labeled glucose. Differences between A- and D-optimal designs were more pronounced, although in each case many different solutions for very similar criterion values existed (data not shown). Optimization attempts for paired experiments were more often unsuccessful in reaching a low criterion value (Fig. 3 trace A2 and D2), which might reflect the smaller differences between different substrate choice solutions.

Neither of the substrate combinations of a paired experiment were equivalent to a lone experiment designs. This suggested that a combined optimization of both substrate solutions lead to an optimal complementary design of experiments, which could not have been achieved if the two experiments had been designed sequentially. Compared to a paired experiment design, where the solutions were corners of the multidimensional design cube (Mollney et al., 1999), a single experiment appeared to resemble more of a compromise, containing 50%  $\text{U-}^{13}\text{C}$ -glucose in most designs.

#### 2.6. Partial optimal design

The benefit of a partial optimal design for the minimization of variance for select fluxes was investigated using

Table 3  
Metabolite measurements that were used for optimal label design

Metabolite	Products	Fragment	MMnts	Set
AcCyt	Fatty acids	1–2	3	
AcPl	Fatty acids	1–2	3	
AlaCyt	Alanine	1–3	4	
		2–3	3	
Cit	Citrate	1–6	7	2
Glu	Glutamine	1–5	6	
	Glutamate	1–5	6	
		2–5	5	
	Proline	1–5	6	2
		2–5	5	2
		2–5	5	2
HP		1–6	7	1
	Starch	PE	6	2
		1–6	6	2
		1–5	6	2
		PE	10	2
	Rhamnose	1–4	5	2
		2–6	6	2
OAA	Asx	1–4	5	
		1–2	3	
		2–4	4	
		2–4	4	2
	Threonine	1–4	5	2
		2–4	4	2
	Malate	1–4	5	2
PGA	Serine	1–3	4	2
		2–3	3	2
		1–2	3	2
	Glycine	1–2	3	2
		2	2	2
RP	Ribulose	1–5	6	
Succ	Succinate	1–4	5	2
TP	Glycerol	1–3	4	
Val	Valine	1–5	5	
		2–5	5	
		2–5	5	2
	Basic	Extended		
Measurements	70	167		
Dependencies	15	33		
Independent measurements	55	134		

For each metabolite shown, a number of label measurements (*MMnts*) were derived from fragments of downstream products. Mass fragments contained the entire or part of the carbon backbone, with the carbons numbered. Positional enrichment (PE) data were derived from NMR measurements. Measurements that were used in one of the measurement sets exclusively were marked 1 = basic and 2 = extended in the *set* column. Unmarked measurements were used in both sets. Mass isotope measurements add up to one, inferring that for each fragment one measurement is dependent. Subtraction of the dependencies from number of measurements yields the number of independent measurements for each data set.

vG6PDH and vRub as an example. Partial optimal design simulations using the partial A- and D-criterion ( $A_L$  and  $D_L$ ) were run in parallel with the simulations presented above. These simulations also compared the effect of additional measurements and an additional labeling experiment. The optimal substrate combinations are shown in Fig. 2 with the suffix L. Comparison of Fig. 2A, B and C, D demonstrates the profound effect that tailored optimal designs had on the substrate label. U- $^{13}\text{C}$ -glucose was replaced by 1,2- $^{13}\text{C}$ -glucose and U- $^{13}\text{C}$ -alanine was no longer used.

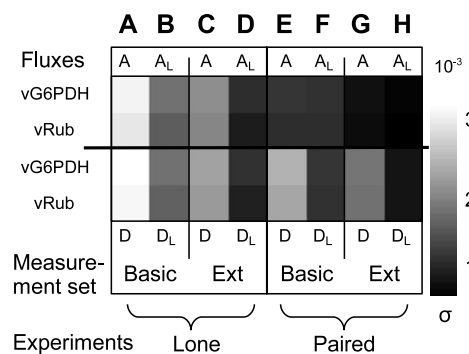


Fig. 4. Comparison of the effects of partial and full A- and D- optimal designs on the standard deviations obtained for two fluxes of interest: vG6PDH and vRub. The full optimal designs are based on taking account of the full set of free fluxes in the network whereas the partial ones only consider the two selected fluxes. Designs (A–H) correspond to the substrate choices shown in Fig. 2 (A–H). Standard deviations of vG6PDH and vRub are shown in the upper and lower squares of each panel, respectively. The upper panels are A-optimal designs and the lower are D-optimal. Within each panel the left column shows a general (A or D), and the right column a partial ( $A_L$  or  $D_L$ ) optimal design. Basic sets of measurements (Basic) are compared to extended datasets (Ext), and lone designs are compared to paired designs. Darker shading shows a lower value of  $\sigma$ , which indicates better definition of a flux value.

Again, A- and D-optimal designs were similar and the additional measurements did not change the substrate combination. For the paired experiment designs 1,2- $^{13}\text{C}$ -glucose was now retained in both experiments and U- $^{13}\text{C}$ -glucose is reduced in the first experiment as well as absent in the second. The use of U- $^{13}\text{C}$ -alanine was also strongly reduced in the  $D_L$ -optimal design and not used at all in the  $A_L$ -optimal design for the extended measurement set.

### 2.7. Partial optimal designs reduce variances of selected fluxes

To investigate the result of the change in substrate label design the information content of the fluxes vG6PDH and vRub was examined in detail (Fig. 4A). The  $\sigma$  values of vG6PDH and vRub are presented in Fig. 4 for the same eight simulations A–H as in Fig. 2. The first column corresponds to simulation A and the last column to experiment H. The first four simulations (single experiments) gave almost identical results for A- and D-optimality, which was expected based on the almost identical substrate solutions for A- and D-optimal designs. Both for the basic and extended measurement set the selective optimal designs  $A_L$  and  $D_L$  greatly improved the information content on the selected two fluxes compared to the general optimal designs using the A- and D-criteria.

For a paired experiment the interpretation was less straight forward. A general D-optimal design performs less well for the two fluxes of interest. A partial optimality was therefore able to greatly improve the information content compared to the general D-optimal design. However, the  $A_L$ -optimal design was hardly an improvement over the A-optimal design. Moreover, the A-optimal design had a

similar performance to the  $D_L$ -optimal design, which made the benefits for a partial optimal design doubtful when designing a paired labeling experiment.

### 2.8. Suppression of large errors in general optimal design

An opposite problem to the partial optimality problem is posed by large variances in the system. A label design for a mutant or other screen should ideally be equally sensitive in all parts of the flux map, suggesting that flux variances should at least be of the same order of magnitude to avoid ‘information holes’. In an attempt to reduce the spread in flux variances,  $\sigma$ s were calculated from the flux covariance matrix and raised to an arbitrary power before summation to form a power weighted A-criterion:  $A^n$ . The effect of this treatment was tried on a single experiment design with basic measurements. The optimization results showing the effect on the largest flux errors are presented ranked by size in Fig. 5. Note that for  $n = 2$  the criterion is the same as for the A-optimal experiment featured in Fig. 2A. The  $\sigma$  of exPPiso (pentose phosphate isomerase), which consistently remained the largest  $\sigma$  with increasing power  $n$ , improved only slightly to the detriment of the other flux  $\sigma$ s. The sum of the flux  $\sigma$ s is depicted above the intensity graph in Fig. 5a. The effect of an increasing power  $n$  on the substrate solution was modest (not shown), and the usefulness of this approach was not evident. The concept of an  $A^n$ -criterion could be useful in certain situations and forms a realistic alternative to the E-criterion in reining in large flux  $\sigma$ s directly,

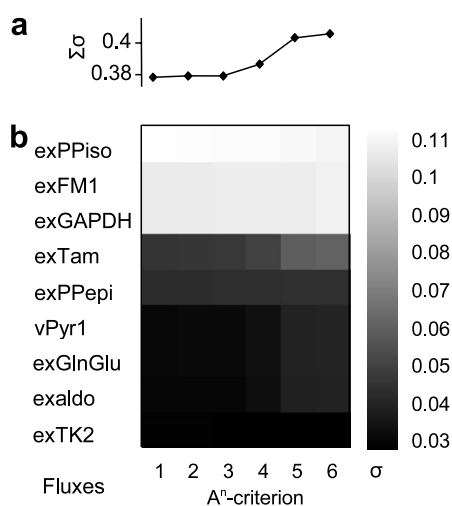


Fig. 5. Comparison of different power-weighted A-optimal designs on the standard deviations of flux estimates. Standard deviations calculated from the covariance matrix were raised to integral powers between 1 and 6 before summation to form an optimal design criterion value  $A^n$ . Higher powers discriminate against large standard deviations. a: The sum of the  $\sigma$  increased with criteria based on higher powers  $n$ . b: Intensity plot for fluxes with  $\sigma$  larger than 0.03. Darker shading shows a lower value of  $\sigma$ , which indicates better definition of a flux value. Increasing powers  $n$  lead to a slight improvement of the largest  $\sigma$  (exPPiso) at the expense of considerable deterioration of the better determined fluxes.

rather than by minimizing the largest axis in the multivariate covariance space.

### 2.9. Comparison of covariances of optimal designs

The optimal design quality criteria used in this study are based on evaluation of the covariance matrix. An optimal design optimizing for the geometric mean  $\sigma^2$  (D-optimality) or the arithmetic mean  $\sigma^2$  (A-optimality) differ in that the D-criterion considers the entire covariance matrix, where the A criterion is only concerned with the  $\sigma^2$  (self covariances located on the diagonal of the covariance matrix). The A- and D-optimal designs were expected to bear out this difference by having smaller inter-flux covariances for the D-optimal design compared to an A-optimal design. However, Comparison of the covariance matrices of an A- and D-optimal design for a two-experiment design with an extended measurement set (Fig. 2G) show very few differences (Fig. 6a). Although the differences in designs had little effect on the appearance of the covariance matrix, the effect on the vG6PDH and vRub fluxes was profound (Fig. 4G). Note that the main difference between the two designs was the addition of 1,2- $^{13}\text{C}$ -glucose to the A-optimal design in the second experiment (Fig. 2G). In the corresponding  $D_L$ -optimal design 1,2- $^{13}\text{C}$ -glucose was also incorporated in the label design (Fig. 2H), confirming the importance of 1,2- $^{13}\text{C}$ -glucose label for the determination of vG6PDH and vRub (Schwender et al., 2004b).

Interpretation of the differences between the A- and  $A_L$ -optimal designs was more straightforward. The small improvement of the  $\sigma^2$  of the fluxes vG6PDH and vRub (Figs. 4A and 6b) came at the expense of a large deterioration (by a factor of 2, data not shown) of the covariances and the mean flux  $\sigma^2$  (Fig. 6b).

### 2.10. $^{13}\text{C}$ in $\text{CO}_2$ determines vG6PDH and vRub

Parameter sensitivity matrices were inspected to see how the influence of measurements over flux estimates changed between a general and partial design (Fig. 6). Note that large parameter sensitivity values imply that small changes in measurements correspond to large changes in the corresponding flux parameters. Conversely, a high parameter sensitivity value for a certain measurement/flux combination indicates that the measurement is *insensitive* to changes in that flux. The A and  $A_L$ -optimal designs of a single experiment design using the basic measurement set were chosen for comparison (Fig. 2A and B). These simulations were chosen because of: (i) the significant improvement of  $A_L$  compared to A for the  $\sigma$ s of vG6PDH and vRub; (ii) the sizable difference in label design; and (iii) the manageable number of measurements for graphing.

A much stronger parameter sensitivity of many measurements of the partial design was apparent (Fig. 7). The columns (fluxes) of the parameter sensitivity matrices that showed the most dramatic increase in sensitivity were fluxes related to the pentose phosphate pathway. The changed

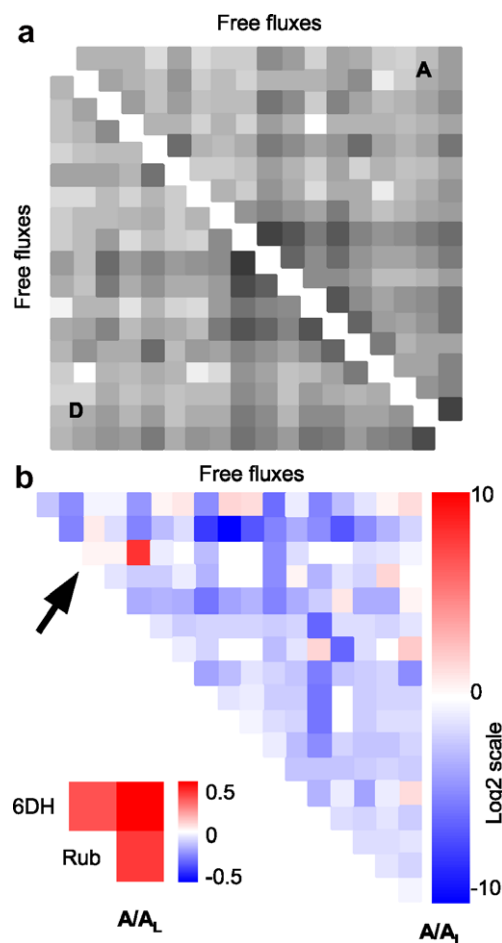


Fig. 6. Free-flux covariance matrices of D- and A-optimal designs. a: Comparison between A- (upper section) and D- (lower section) optimal designs showed only small differences and did not reveal a clear pattern. Since the covariance matrices are symmetrical only half the matrix in addition to the diagonal are shown in each case. The grayscale is scaled from the smallest to the largest value and intensities are shown on a logarithmic scale. b: Comparison of a general to a partial A-optimal design clearly demonstrated the high cost incurred on covariances of most of the fluxes for a marginal improvements of vG6PDH and vRub. Only vG6PDH (arrow) is shown on the diagonal of the main triangle because vRub was defined as a dependent flux and thus does not appear in the free flux covariance matrix. Inset shows an illustration of the relative change in the covariances for vRub and vG6PDH.

measurements were positioned close to CO<sub>2</sub> releasing steps, indicating that measurements sensitive to CO<sub>2</sub> label had been ‘uncoupled’ from PPP fluxes that had large  $\sigma$ .

Inspection of the corresponding measurement sensitivity matrices (data not shown) indicated that measurements of labeling in oxaloacetate (OAA) were more sensitive to flux changes in the partial design. Only the free net fluxes vG6PDH and vFM were found to be better determined by measurements. The higher sensitivity of measurements to vG6PDH was to be expected given that this flux was optimized for.

The combined information above suggested that the increased information content for vG6PDH and vRub for the A<sub>L</sub>-optimal design was accomplished by: (i) reduc-

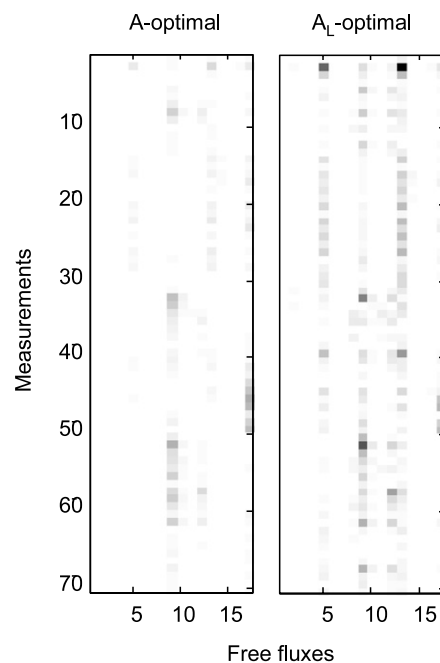


Fig. 7. Flux parameter sensitivity of a partial and general A-optimal design. The flux sensitivity to label measurements for the partial optimal design, which was selective for vRub and vG6PDH, was greatly increased. Darker shading indicates higher sensitivity of fluxes to label measurements. Closer inspection revealed that measurements close to fluxes related to CO<sub>2</sub> release had become less responsive to fluxes in the pentose phosphate pathway. The reduced dependency of metabolites reporting on label in CO<sub>2</sub> on the poorly determined pentose phosphate pathway increased the precision of the estimate of label in CO<sub>2</sub>. Consequently, this resulted in a better estimate of the CO<sub>2</sub> releasing flux vG6PDH and the CO<sub>2</sub> incorporating flux vRub.

tion of the dependence of the CO<sub>2</sub> label on poorly determined fluxes; (ii) increasing the precision of CO<sub>2</sub> label measurements through OAA and; (iii) increasing the sensitivity of label measurements to the two fluxes adjacent to OAA. This explained the somewhat counterintuitive result that to improve the determination of vG6PDH and vRub, the TCA cycle flux vFM had improved, where the  $\sigma$ s of most PPP fluxes had worsened. Despite the importance of CO<sub>2</sub> label in determining a flux map, CO<sub>2</sub> itself is not a suitable substrate for steady state experiments. *Brassica* embryos are net CO<sub>2</sub> producers, which results in a build-up of CO<sub>2</sub> (Goffman et al., 2004). Metabolically produced CO<sub>2</sub> will carry a different label than the hypothetical input label, and result in a label gradient within the embryo and a change of label in CO<sub>2</sub> during the experiment. Both of these effects violate the steady state assumptions, and the use of labeled amino acids as <sup>13</sup>CO<sub>2</sub> donors is therefore a good alternative.

### 2.11. Reparameterization of an optimal design

An optimal design is determined for a given flux combination and the quality of the label design is sensitive to changes in the fluxes. This property deserved careful consideration because an optimal design is based on flux *estimates* and because the label design must still be useful

after significant flux changes if it is to be useful for comparing two flux maps. From optimal design theory a D-optimal design is known to be least sensitive to parameter change (Pázman, 1986). However, D-criterion values are poor predictors of arithmetic means (compare  $I_D$  to  $I_A$  or  $I_\sigma$  values in Table 2). Simulation of large parameter changes often resulted in infeasible free flux combinations, which prevented systematic analysis of sensitivity to parameter change.

In an example simulation the CO<sub>2</sub> output flux was reduced by 50% relative to the substrate uptake rate, which is equivalent to an increase in carbon conversion efficiency (Goffman et al., 2005). To maintain the stoichiometric balance of the network, this change resulted in a reduction of flux through glycolysis, compensated for by an increase in flow through vRub and the non-oxidative part of the pentose phosphate pathway. This set of compensatory changes is a reflection of the arbitrarily choice of which fluxes are treated as free fluxes and is by no means unique and is thus not predictive. The stability of the optimal design was investigated for a single experiment design using the extended measurement set (Fig. 2E). This case was chosen because of the considerable differences in substrate label between the A- and D-optimal designs. In this case the D-optimal design also had a better D-criterion value than the A-optimal design (data not shown), which was not the case for all simulations (Table 2).

Both A- and D-optimal designs showed a reduction in  $I_\sigma$  and  $I_A$  (with the criterion values prior to change chosen as reference) in response to the smaller CO<sub>2</sub> efflux, which shows that a change in parameter value does not necessarily lead to an increase in variance. The D-criterion was more stable for both optimal designs (<5% change). However contrary to the arithmetic comparisons  $I_\sigma$  and  $I_A$ , the  $I_D$  had increased in response to the reduced CO<sub>2</sub> efflux. This confirmed that the D-criterion is a poor predictor of the arithmetic mean. Although the  $I_\sigma$  and  $I_A$  for the D-optimal design both improved more than for the A-optimal design, the  $\bar{\sigma}$  and mean of  $\sigma^2$  of the A-optimal design were still substantially better. The stability of the D-optimal design might translate into better performance when very large parameter changes are to be expected.

### 3. Conclusions

The optimal substrate designs were distinctly different from substrate labeling designed for bacterial cultures taken from the literature (Fig. 2). The large difference between the designs lead to a much better (~5-fold) performance of designs for the *B. napus* network by all evaluation criteria (Table 2). The information content was further improved by a factor of ~2.5 by increasing the amount of label measurements and by performing a paired experiment, both contributing roughly equally. Simulated variances of specific fluxes could be even further reduced by specifically optimizing for these fluxes.

The choice of optimality criterion is not straight forward and the statistical behavior in response to parameter change cannot be predicted easily.

The optimization trials produced many experimental designs that had very similar criterion values (Fig. 3) but substantially different substrate compositions. Together with the notion that both D- and A-optimal designs have specific beneficial qualities, a substrate design that performs well for both criteria should be a substrate solution of choice. In practice many such solutions were found and a substrate choice should rarely have to compromise by more than 1% for either criterion. In the specific case where flux values are well determined already and little change in flux values is expected, the A-optimal solution should probably be preferred. Because of the variety of roughly equivalent optimal solutions, the different price of substrates is also a valid consideration.

For mutant screens, where equal variance i.e. homogeneous coverage for the entire map is the priority, the sum of power weighted individual  $\sigma_s$  (Fig. 4B) or an E-optimal design should be considered.

Although here suggested optimal label designs are likely to perform better on other plant systems than designs used for bacterial cultures, plant cultures greatly vary in their carbon uptake and customized designs are likely to yield significant benefits.

## 4. Experimental

### 4.1. Network definition and measurements

The metabolic network definition, mass-spectroscopy measurements and flux estimates were taken from Schwender et al. (2006). Additional measurements have since been developed and implemented (Allen et al., 2007). Only a subset, which could be implemented without change in the network definition have been used in this paper (Table 3).

Fluxes to biomass, as well as fluxes that were unidentifiable in the original flux map were fixed and the associated variance was therefore not considered. The same fluxes, although now measurable, were fixed when the extended measurement set was used for fair comparison.

### 4.2. Optimal design criteria

A criterion value is a function of the substrate label  $x^{\text{inp}}$ , the measurement set  $M_y$  and the flux parameter values  $\Theta$ .

$$\text{crit}(x^{\text{inp}}, M_y, \Theta) = \text{evaluation of Cov}(x^{\text{inp}}, M_y, \Theta)$$

For an optimal design using a given criterion, the criterion value of interest is minimized by finding the optimal feasible substrate combination  $x_{\text{feasible}}^{\text{inp}}$ , using the measurement set and the flux parameters  $\Theta$ .

$$\text{crit}_{\text{opt}}(\Theta) = \min_{x_{\text{feasible}}^{\text{inp}}, M_y} \text{crit}(x^{\text{inp}}, M_y, \Theta)$$

The D-criterion is the most frequently used quality criterion and has already been implemented successfully in optimal label design studies for microbial systems (Arauzo-Bravo and Shimizu, 2003; Mollney et al., 1999). The D-criterion is calculated from the determinant of the covariance matrix, which can be interpreted as a volume of an ellipsoid spanning the entire variance of the parameter space. The determinant of the covariance matrix has a direct relationship to the geometric mean of the variance  $\sigma^2$  of the parameter estimates because it is described by the multiplication of the eigenvalues of the covariance matrix. To scale the determinant to the geometric mean of  $\sigma$  ( $\bar{\sigma}$ ) for comparison to the arithmetic mean of  $\sigma$  ( $\bar{\sigma}$ ), the D-criterion is defined as:

$$D_{\text{crit}} = \sqrt[2n]{\det(\text{Cov})}$$

Note that the  $2n$ th, rather than the  $n$ th root is taken to relate to the  $\bar{\sigma}$  rather than to the mean of  $\sigma^2$ .  $n$  is the number of fluxes considered, which is equal to the number of eigenvalues. Because the product of the eigenvalues is smallest when the largest and smallest eigenvalues differ most, the shape of the ellipsoid described by the D-criterion tends to become needle like. The more needle-shaped this ellipsoid becomes; the greater the difference is between the geometric and arithmetic mean.

The A-criterion is simply the sum of the diagonal elements of the covariance matrix (trace). For consistency with the  $D_{\text{crit}}$ , the criterion value is scaled to ( $\bar{\sigma}$ ) by taking the root of the A-criterion divided by the number of fluxes considered.

$$A_{\text{crit}} = \sqrt{\frac{\text{tr}(\text{Cov})}{n}}$$

The ( $\bar{\sigma}$ ) is also calculated directly from the covariance matrix, taking the sum of the square roots of the diagonal elements of the covariance matrix.

The E-criterion value is the largest eigenvalue of the covariance matrix. By minimizing the value of the largest eigenvalue the maximum variance along one principal component axis of the covariance matrix is minimized. However, the largest eigenvalue bears no direct relationship to the largest parameter  $\sigma^2$ , but merely limits its value. Therefore an E-criterion value cannot be compared to a mean of  $\sigma$  directly.

#### 4.3. Partial optimality criteria

To consider only a subset of fluxes  $s$  for a criterion calculation of an  $m \times m$  covariance matrix  $A$ ,  $A$  was partitioned into submatrices  $A = \begin{bmatrix} A_I & A_{II} \\ A'_{II} & A_{III} \end{bmatrix}$  so that  $A_I$  was the  $s \times s$  subcovariance matrix  $\text{Cov}_L$ . Partial criteria were then calculated from  $\text{Cov}_L$  as before (Pázman, 1986).

#### 4.4. Flux and measurement errors

A measurement error contains both an absolute and a relative component, where absolute errors correspond to

technical issues, and biological variability underlies relative errors. Because the small number of samples in flux experiments can lead to very unreliable estimates of the true  $\sigma$ , technical errors are often employed instead (Mollney et al., 1999). Biological variability can be reliably estimated by repeating the experiments many times ( $n > 30$ ), though this is rarely if ever done in steady state labeling studies. Absolute errors are even harder to estimate. Although the sensitivity and reproducibility of the analytical measurements can be readily determined, systematic errors such as wash out errors are impossible to gauge accurately.

In this simulation individual errors were simulated using a relative (biological) error of 1% of the measurement value and an absolute error of 0.1%. The relative errors will not by themselves change the label design since they will merely scale the errors on the flux estimates. The absolute errors will affect the label design solution, and the size of the absolute errors is a crude estimate at best. Where in previous work different values were assigned for Mass-spectroscopy and NMR measurements (Mollney et al., 1999) this distinction was not made in this study, because the signal to noise for NMR measurements is largely under the control of the experimenter.

#### 4.5. Criterion computation

The D-criterion was derived by taking the  $2n$ th root of the determinant of the covariance matrix, where  $n$  is the number of fluxes considered. The determinant from the covariance matrix was either determined directly using Octave (Eaton, 2002) or through singular value decomposition of the covariance matrix followed by multiplication of the eigenvalues. The E-criterion was determined by selecting the largest eigenvalue after singular value decomposition of the covariance matrix.

The A-criterion was calculated by taking the square root of the trace (sum of the diagonal elements) of the covariance matrix divided by the number of elements. An  $n$  power weighted A-criterion was calculated by raising the square roots of the individual elements of the covariance matrix to the  $p$ th power prior to summation, followed by taking the  $p$ th root. The  $\bar{\sigma}$  was calculated dividing the power weighted A-criterion ( $p = 1$ ) through the number of considered fluxes.

#### 4.6. Optimizations

Optimizations were performed using the GNU software Donlp2 (Spellucci, 1998). The programs CumoNet, ResiduumScanner and EstimStat of the  $^{13}\text{C}$ -flux suite (obtained from W. Wiechert, Siegen University) were used to simulate measurements and calculate the flux covariance matrix. Custom written Perl scripts were used to automate the calls to the  $^{13}\text{C}$ -flux programs and analyze the output for Donlp2. A-, D- and E-optimality are all concave and therefore suitable for optimization purposes. All software ran on RedHat Linux installed on typical desktop

PCs. Optimizations were initiated from random substrate combinations and typically took a few hours per optimization.

### Acknowledgements

The authors thank Professor F. Pukelsheim (Augsburg University) for his expert advice on optimal design, Professors W. Wiechert (Siegen University) and D. Gilliland (MSU) and Dr. K. Nöh (Siegen University) for critically reading the manuscript. We acknowledge Mochan Shrestha and Dave Girdwood (MSU) for coding, and Drs. Doug Allen and Ana Alonso (MSU) for helpful discussion and the USDA-NRI for funding this work.

### References

- Allen, D.K., Shachar-Hill, Y., Ohlrogge, J.B., 2007. Compartment-specific labeling information in  $^{13}\text{C}$  metabolic flux analysis of plants. *Phytochemistry*, this issue. doi:10.1016/j.phytochem.2007.04.010.
- Arauzo-Bravo, M.J., Shimizu, K., 2003. An improved method for statistical analysis of metabolic flux analysis using isotopomer mapping matrices with analytical expressions. *Journal of Biotechnology* 105, 117–133.
- Eaton, J.W., 2002. Gnu Octave Manual. Network Theory Ltd.
- Fischer, E., Sauer, U., 2003. Metabolic flux profiling of *Escherichia coli* mutants in central carbon metabolism using GC–MS. *European Journal of Biochemistry* 270, 880–891.
- Goffman, F.D., Alonso, A.P., Schwender, J., Shachar-Hill, Y., Ohlrogge, J.B., 2005. Light enables a very high efficiency of carbon storage in developing embryos of rapeseed. *Plant Physiology* 138, 2269–2279.
- Goffman, F.D., Ruckle, M., Ohlrogge, J., Shachar-Hill, Y., 2004. Carbon dioxide concentrations are very high in developing oilseeds. *Plant Physiology and Biochemistry* 42, 703–708.
- Mollney, M., Wiechert, W., Kownatzki, D., de Graaf, A.A., 1999. Bidirectional reaction steps in metabolic networks: IV. Optimal design of isotopomer labeling experiments. *Biotechnology and Bioengineering* 66, 86–103.
- Pázman, A., 1986. Foundations of Optimum Experimental Design. D. Reidel, Dordrecht, Holland.
- Pukelsheim, F., 1993. *Optimal Design of Experiments*. Wiley, New York.
- Ratcliffe, R.G., Shachar-Hill, Y., 2006. Measuring multiple fluxes through plant metabolic networks. *Plant Journal* 45, 490–511.
- Sauer, U., 2006. Metabolic networks in motion: C-13-based flux analysis. *Molecular Systems Biology* 2, 62, doi:10.1038/msb4100109.
- Schmidt, K., Carlsen, M., Nielsen, J., Villadsen, J., 1997. Modeling isotopomer distributions in biochemical networks using isotopomer mapping matrices. *Biotechnology and Bioengineering* 55, 831–840.
- Schwender, J., Goffman, F.D., Ohlrogge, J.B., Shachar-Hill, Y., 2004a. Rubisco without the Calvin cycle improves the carbon efficiency of developing green seeds. *Nature* 432, 779–782.
- Schwender, J., Ohlrogge, J.B., Shachar-Hill, Y., 2004b. Understanding flux in plant metabolic networks. *Current Opinion in Plant Biology* 7, 309–317.
- Schwender, J., Shachar-Hill, Y., Ohlrogge, J.B., 2006. Mitochondrial metabolism in developing embryos of *Brassica napus*. *Journal of Biological Chemistry* 281, 34040–34047.
- Spellucci, P., 1998. An SQP method for general nonlinear programs using only equality constrained subproblems. *Mathematical Programming* 82, 413–448.
- Szyperki, T., 1995. Biosynthetically directed fractional C-13-labeling of proteinogenic amino-acids – an efficient analytical tool to investigate intermediary metabolism. *European Journal of Biochemistry* 232, 433–448.
- van Winden, W.A., Heijnen, J.J., Verheijen, P.J.T., Grievink, J., 2001. A priori analysis of metabolic flux identifiability from C-13-labeling data. *Biotechnology and Bioengineering* 74, 505–516.
- Wiechert, W., de Graaf, A.A., 1997. Bidirectional reaction steps in metabolic networks. I. Modeling and simulation of carbon isotope labeling experiments. *Biotechnology and Bioengineering* 55, 101–117.
- Wiechert, W., Mollney, M., Isermann, N., Wurzel, W., de Graaf, A.A., 1999. Bidirectional reaction steps in metabolic networks: III. Explicit solution and analysis of isotopomer labeling systems. *Biotechnology and Bioengineering* 66, 69–85.
- Wiechert, W., Siefke, C., de Graaf, A.A., Marx, A., 1997. Bidirectional reaction steps in metabolic networks. II. Flux estimation and statistical analysis. *Biotechnology and Bioengineering* 55, 118–135.
- Wittmann, C., Heinzle, E., 2001. Modeling and experimental design for metabolic flux analysis of lysine-producing *Corynebacteria* by mass spectrometry. *Metabolic Engineering* 3, 173–191.